



Contents lists available at ScienceDirect

## Microelectronic Engineering

journal homepage: [www.elsevier.com/locate/mee](http://www.elsevier.com/locate/mee)

## Optimization of illumination pupils and mask structures for proximity printing

K. Motzek<sup>a,\*</sup>, A. Bich<sup>b</sup>, A. Erdmann<sup>a</sup>, M. Hornung<sup>c</sup>, M. Hennemeyer<sup>c</sup>, B. Meliorisz<sup>d</sup>, U. Hofmann<sup>d</sup>, N. Ünal<sup>d</sup>, R. Voelkel<sup>b</sup>, S. Partel<sup>e</sup>, P. Hudek<sup>e</sup><sup>a</sup>Fraunhofer IISB, Schottkystr. 10, 91058 Erlangen, Germany<sup>b</sup>SUSS MicroOptics SA, Rue Jaquet-Droz 7, 2000 Neuchatel, Switzerland<sup>c</sup>SUSS MicroTec Lithography GmbH, Schleissheimer Str. 90, 85748 Garching, Germany<sup>d</sup>GenSys GmbH, Eschenstr. 66, 82024 Taufkirchen, Germany<sup>e</sup>Vorarlberg University of Applied Sciences, Hochschulstrasse 1, 6850 Dornbirn, Austria

## ARTICLE INFO

## Article history:

Received 11 September 2009

Accepted 28 October 2009

Available online xxx

## Keywords:

Optical lithography

Mask aligner

Proximity printing

Illumination pupil

Optical proximity correction

MO exposure optics

## ABSTRACT

Based on numerical simulations, we show the influence of the illumination on process windows in mask aligner lithography. The precise shaping of the illuminating light can lead to greatly increased process windows. We show that the best results are obtained when combining an optimized illumination with optimized mask structures and Optical Proximity Correction (OPC). We model the illumination according to the novel illumination system for SUSS MicroTec mask aligners, referred to as MO Exposure Optics, which allows a precise shaping of the angular spectrum and the partial coherence of the mask illuminating light by using Illumination Filter Plates (IFPs).

© 2009 Elsevier B.V. All rights reserved.

## 1. Introduction

The illumination has a major impact on the outcome of any optical lithographic process [1]. A lot of the progress made in projection printing with high-end photolithography systems in recent years can be attributed to the use of tailored pupils for processes near the resolution limit. The rapid growth of the field of source-mask-optimization demonstrates the importance of the illumination for creating the smallest structures currently manufacturable by means of optical lithography [2,3]. Outside the realm of high-end projection lithography systems, however, there were very little possibilities for the users to adjust the angular spectrum and partial coherence of the mask illuminating light to their processes until the novel illumination system for SUSS MicroTec mask aligners, referred as MO Exposure Optics, was introduced a few months ago. The MO Exposure Optics allows the users to define the angular spectrum by Illumination Filter Plates (IFPs). The IFPs are stops inserted into the pupil plane of the illumination system. Therefore, the angular spectrum defined by the IFP can be compared to the illumination pupil in projection lithography. In the following, we will use the term 'illumination pupil' as a synonym for the angular spectrum of the mask illuminating light defined by the IFP.

Based on numerical simulations of mask proximity printing [4,5], this paper aims at showing how changes to the illumination pupil (i.e. to the IFP) will affect the process window and how strongly an optimized pupil can increase the size of a process window. Also, we will show that the best results are obtained by a combination of optimizing the pupil and applying changes to the mask structures.

## 2. Numerical approach

For our simulations we assumed a 3 μm thick resist (with a refractive index of 1.69 and an extinction coefficient of 0.005) on a silicon substrate. The optical part of the simulations was performed using scalar diffraction analysis [4,6]. We used a simple threshold model for resist development. The threshold model was applied to the light intensity integrated over the propagation direction in the area between 0.15 and 0.45 μm above the interface between resist and substrate, as this area has the strongest impact on the resulting resist profile upon development.

In the numerical optimization of the illumination we used different types of IFP with geometries that can be described by a small set of parameters. The angular spectra of the mask illuminating light produced by the most important ones are shown in Fig. 1.

The influence of the illumination pupil on the printing process can be most easily studied and understood when using

\* Corresponding author.

E-mail address: [kristian.motzek@iisb.fraunhofer.de](mailto:kristian.motzek@iisb.fraunhofer.de) (K. Motzek).

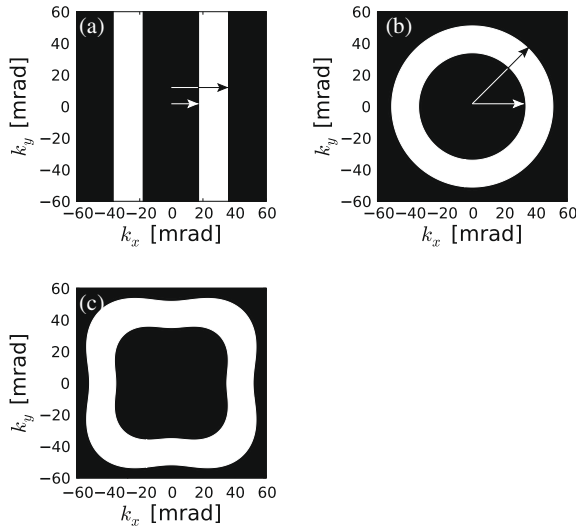


**Fig. 1.** The pictures show the angular spectra of the mask illuminating light produced by the different types of IFPs we tested in the optimization process. We use the transverse components of the light's wave vector ( $k_x$  and  $k_y$ ) to describe the illumination angles. (a) shows a pupil that contains light only where the modulus of  $k_x$  lies between a minimal value  $k_{min}$  and a maximal value  $k_{max}$  (indicated by the arrows). The annular IFP in (b) contains light only where the modulus of the transverse wave vector  $(k_x^2 + k_y^2)^{1/2}$  lies between  $k_{min}$  and  $k_{max}$ . The IFP shown in (c) is described by three parameters: the inner ( $r_i$ ) and outer radius ( $r_o$ ) of the ring are modulated over the azimuth like  $r_i(\varphi) = k_{min}(1 + \zeta \cos(4\varphi))$  and  $r_o(\varphi) = k_{max}(1 + \zeta \cos(4\varphi))$ , where  $\zeta$  is a measure for the deviation from the annular form.

monochromatic light. All simulations were therefore performed assuming a monochromatic light source of wavelength 365 nm.

**3. Results**

The first problem we investigated was the printing of 2  $\mu$ m wide bright lines with a semi-dense pitch of 8  $\mu$ m at a proximity gap around 20  $\mu$ m. The difficulties encountered when trying to print such lines using a mask that consists of 2  $\mu$ m bright lines can be explained by taking a look at Fig. 2. Fig. 2a shows the intensity profile obtained with a plane wave illumination at a proximity gap of 20  $\mu$ m. The multitude of local minima and maxima caused

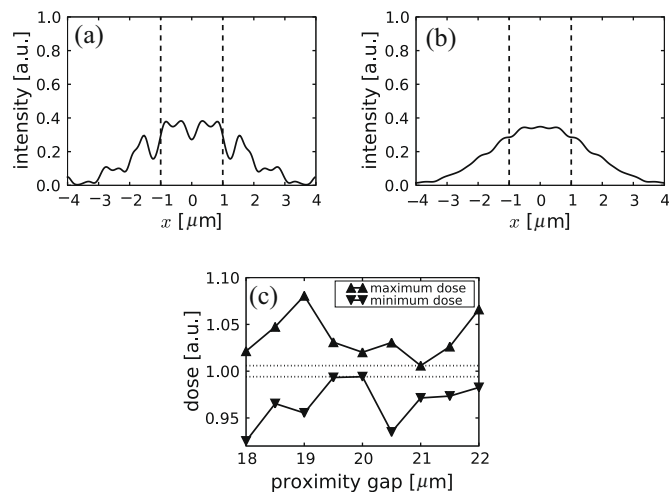


**Fig. 2.** (a) Shows the intensity profile at a proximity gap of 20  $\mu$ m obtained with a mask consisting of 2  $\mu$ m semi-dense lines using a plane wave as illumination. Using an optimized IFP, the intensity profile looks more favorable, as shown in (b). The process window obtained when using the optimized IFP is shown in (c).

by diffraction makes it impossible to print 2  $\mu$ m lines with such a configuration.

We used an optimization algorithm to look for an IFP that would generate the biggest possible process window for a mask with 2  $\mu$ m lines. The process window is defined as the maximum dose variation that will produce results within specification [4] (it is commonly assumed that a structure is within specification if it does not deviate more than 10% from the targeted size). The robustness of a process against dose variations is important, because the dose can only be controlled with a certain precision and because the dose varies over the wafer due to inhomogeneities in the illumination system. Since not only the dose but also the proximity gap can only be controlled with a certain precision, a robust process needs to allow dose variations over a range of gaps. We assumed that the proximity gap can be controlled with a precision of  $\pm 2 \mu$ m and therefore calculated the process window between 18.0 and 22.0  $\mu$ m.

The type of IFP we optimized is shown in Fig. 1a. As a result of the optimization, we obtained values for  $k_{max}$  of 25 mrad and for  $k_{min}$  of 0 mrad (i.e. the two bright stripes in Fig. 1a merge into one). The intensity profile at a proximity gap of 20  $\mu$ m obtained with that IFP is shown in Fig. 2b and the process window is shown in Fig. 2c. Doses in Fig. 2c were normalized to the optimum dose for that process. The process window is the area between the two dotted horizontal lines. The maximum dose variations allowed are less than 1%. Under realistic conditions such a process is therefore infeasible.

To obtain a better process window, we next optimized not only the pupil, but also the width of the lines on the mask. Again, the type of IFP optimized is shown in Fig. 1a. We now have to optimize three parameters simultaneously: two parameters ( $k_{max}$  and  $k_{min}$ ) describing the IFP and the line width on the mask. Our optimization algorithm found the largest process window for a linewidth of 2.9  $\mu$ m on the mask and a pupil with  $k_{max} = 45$  mrad and  $k_{min} = 0$  mrad.

Fig. 3a shows the intensity profile produced with a mask with 2.9  $\mu$ m lines at a proximity gap of 20  $\mu$ m using a plane wave as illumination. It is not suitable for printing 2  $\mu$ m lines either. However, Fig. 3b shows the profile obtained when using the optimized IFP and Fig. 3c shows the resulting process window. Here, dose variations of  $\pm 7\%$  are allowed, making it much more likely that such a process could work in reality.

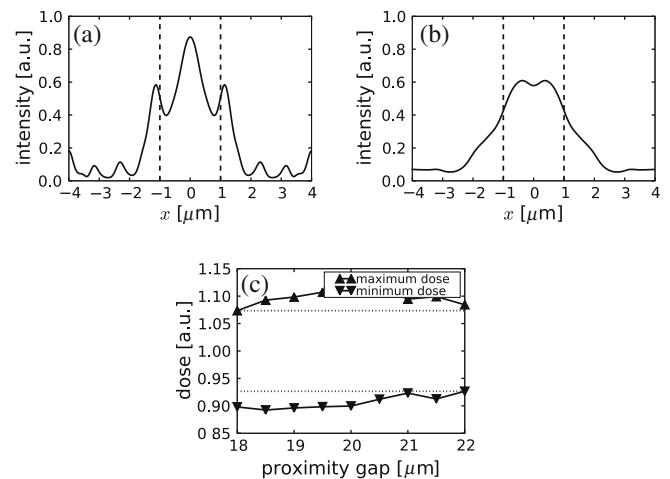


**Fig. 3.** (a) Shows the intensity profile at a proximity gap of 20  $\mu$ m obtained with a mask consisting of 2.9  $\mu$ m lines and a pitch of 8  $\mu$ m using a plane wave as illumination. The intensity profile obtained when using an optimized IFP is shown in (b). The corresponding process window is shown in (c).

Our next aim was to print  $5\ \mu\text{m}$  posts with a pitch of  $20\ \mu\text{m}$  at proximity gaps around  $33\ \mu\text{m}$ . To calculate a process window, we defined that any result would be within specification if the footprint of the post lies entirely between a square of  $4.5\ \mu\text{m}$  and a square of  $5.5\ \mu\text{m}$  edge length.

Again, the simulations show that a plane wave illumination would not be suitable for printing posts of that size at this relatively large proximity gap. We therefore used the type of IFP shown in Fig. 1b and optimized the values of  $k_{\min}$  and  $k_{\max}$ , describing the inner and outer radius of the annulus.

First, we assumed an ‘unoptimized’ mask, i.e. the mask looks like the structure we are trying to print ( $5\ \mu\text{m}$  squares with a pitch of  $20\ \mu\text{m}$ ). With the mask being fixed, we only have two parameters to optimize:  $k_{\min}$  and  $k_{\max}$ . We found the largest process window for  $k_{\min} = 40\ \text{mrad}$  and  $k_{\max} = 55\ \text{mrad}$ .

To demonstrate the importance of choosing the right IFP on the result of the printing process, Fig. 4a shows the footprint of the post at a proximity gap of  $33\ \mu\text{m}$  obtained when using a ‘wrong’ IFP with  $k_{\min} = 0\ \text{mrad}$  and  $k_{\max} = 55\ \text{mrad}$ . (Note that this results in an angular spectrum of the mask illuminating light similar to the one currently used in many mask aligner systems.) The footprint of the post obtained when using the optimized IFP is shown in Fig. 4b. It resembles much more the square profile that we targeted at. The process window with optimized IFP is shown in Fig. 4c.

Again, we can increase the size of the process window considerably if we modify the structures on the mask. Varying the size of the squares on the mask did not have any beneficial effects. Instead, we used assist structures to come to bigger process windows. Inspired by the rules for optical proximity correction (OPC) in projection lithography, we added little squares at the corners of our  $5\ \mu\text{m}$  square and optimized the size of these assist structures together with the parameters describing the IFP. The result we got was the mask structure shown in Fig. 5d. The type of IFP used in the optimization is shown in Fig. 1c (in fact, Fig. 1c shows the optimized pupil). The parameters we obtained for the pupil were  $k_{\min} = 35\ \text{mrad}$ ,  $k_{\max} = 57\ \text{mrad}$  and  $\xi = -0.11$ .

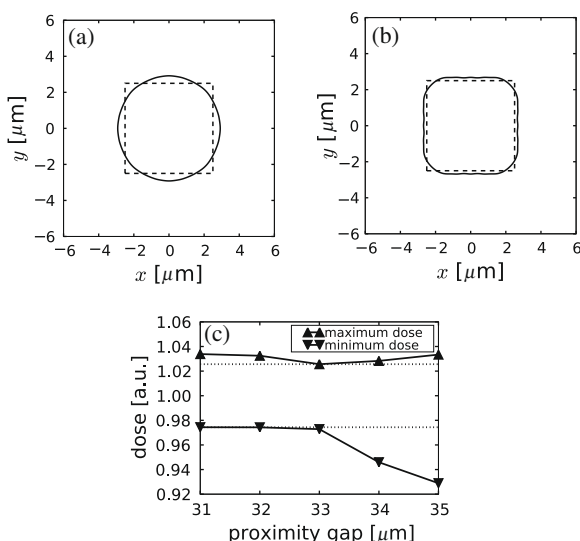


**Fig. 4.** The figures show the simulation results of printing  $5\ \mu\text{m}$  posts with an ‘unoptimized’ mask. The solid line in (a) shows the footprint obtained at a proximity gap of  $33\ \mu\text{m}$  when using an annular IFP that has not been optimized either. (Here,  $k_{\min} = 0\ \text{mrad}$  and  $k_{\max} = 55\ \text{mrad}$ .) The dashed square is the  $5\ \mu\text{m}$  square we want to print. The footprint obtained when using the optimized IFP ( $k_{\min} = 40\ \text{mrad}$  and  $k_{\max} = 55\ \text{mrad}$ ) is shown in (b). The corresponding process window is shown in (c).

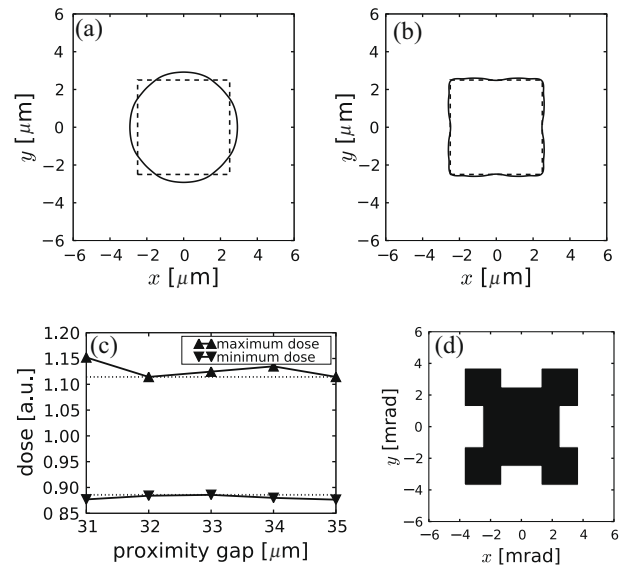


**Fig. 5.** The figures show the simulation results of printing  $5\ \mu\text{m}$  posts with an optimized mask. The solid line in (a) shows the footprint obtained at a proximity gap of  $33\ \mu\text{m}$  when using the optimized mask layout without using the co-optimized IFP. The footprint obtained when using the optimized IFP is shown in (b). The corresponding process window is shown in (c). The optimized mask structure is shown in (d). It consists of a large square with edge length  $5\ \mu\text{m}$  and four small squares of edge length  $1.2\ \mu\text{m}$  centered around the corners of the big square.

Again, to emphasize the importance of the IFP, we calculated the footprint of the post at  $33\ \mu\text{m}$  using a wrong IFP (annular with  $k_{\min} = 0\ \text{mrad}$  and  $k_{\max} = 55\ \text{mrad}$ ). Fig. 5a shows that the footprint strongly deviates from the targeted square profile, despite the assist structures on the mask. When using the optimized IFP the footprint of the post is an almost perfect  $5\ \mu\text{m}$  square, as shown in Fig. 5b. The process window for the optimized solution is shown in Fig. 5c.

The comparison between the process windows and footprints in Figs. 4 and 5a and b show the benefit of using OPC structures to the mask. However, this means that we have to parameterize the shape of the pupil and the structures on the mask and that the number of parameters included in our optimization increases. Future investigations will have to show how many free parameters are really needed in the optimization to come to satisfying results.

#### 4. Conclusion

In conclusion, we have shown the essential role of the illumination pupil for mask aligner lithography and how the adequate choice of an IFP can open process windows that are otherwise non-existent. Even more powerful is the combination of OPC and an optimized IFP.

To use our numerical findings practically, one will have to take into consideration in much detail the properties of the light source, the bleaching of the resist and possibly other effects as well. An in-depth investigation of these effects as well as the extension of the results presented here to more complicated structures and pupils and the comparison with experimental data is a task that will most probably help to extend the limits of mask aligner lithography.

#### Acknowledgments

The authors would like to thank the Bayerische Forschungsstiftung for funding this work in the framework of the project ‘MALS’.

**References**

- [1] A.E. Rosenbluth, S. Bukowski, M. Hibbs, K. Lai, A. Molles, R. Singh, A.K. Wong, Proc. SPIE 4346 (2001) 486.
- [2] T. Fühner, S. Popp, C. Dürr, A. Erdmann, Proc. SPIE 6154 (2006) 1269.
- [3] A.E. Rosenbluth, D.O. Melville, K. Tian, S. Bagheri, J. Tirapu-Azpiroz, K. Lai, A. Waechter, T. Inoue, L. Ladanyi, F. Barahona, K. Scheinberg, M. Sakamoto, H. Muta, E. Gallagher, T. Faure, M. Hibbs, A. Tritchkov, Y. Granik, Proc. SPIE 7274 (2009) 727409.
- [4] B. Meliorisz, P. Evanschitzky, A. Erdmann, *Microelectron. Eng.* 84 (2007) 733.
- [5] W. Henke, M. Weiss, R. Schwalm, J. Pelka, *Microelectron. Eng.* 10 (1990) 127.
- [6] J.D. Jackson, *Classical Electrodynamics*, John Wiley and Sons, 1975.